A Wideband Circularly Polarized Microstrip Antenna With Multiple Modes

LEI WANG [1,2] (Member, IEEE), AND YUN-FEI EN [1] (Senior Member, IEEE)

[1] China Electronic Produce Reliability and Environmental Testing Research Institute, Guangzhou 510610, China

[2] Xidian University, Xi'an 710071, China

CORRESPONDING AUTHOR: Y.-F. EN (e-mail: enyf@ceprei.com)

ABSTRACT A new compact wideband circularly polarized (CP) antenna is proposed in this work. The antenna consists of a CP square-loop with sequential phase (SP) characteristics, four strip-lines as driven elements, four L-shaped patches with I-slots and four I-shaped patches as parasitic elements. The square-loop is utilized to feed the two pairs of parasitic patch arrays by a capacitively coupled way. The proposed antenna has a broad 3-dB axial ratio bandwidth (ARBW) of 18.9% (6.35 GHz, 5.75-6.95 GHz), and a wide 10-dB impedance bandwidth (IBW) of 23% (6.38 GHz, 5.65-7.12 GHz). Besides, the presented antenna features flat gain within the CP operation bandwidth and compact structure.

INDEX TERMS Broadband antenna, circularly polarized antenna, parasitic patch.

I. INTRODUCTION

OWING to the outstanding features of improving polarization mismatch and eliminating multipath distortion than linear-polarization, circular-polarization (CP) is massively adopted in satellite and mobile communications [1]–[2]. In addition, CP microstrip patch antennas (MPA) [3]–[24] are extremely attractive over the years due of their excellent features of low cost, low profile, and easy integration. However, narrow circular-polarization bandwidth (CPBW) is one of the most challenges for CP MPA in the application of wireless communication systems.

It is well known that the sequential rotate technique (SRT) has been widely used in the design of CP antenna [3]–[22]. A 4 × 4 CP slot antenna array is designed by combining SRT with the substrate-integrated waveguide technique in [4], which obtains 14% axial ratio bandwidth (ARBW). Since the CP elements have narrow ARBW, the SRT feeding network is adopted to improve the ARBW of the antenna array in [5]–[6]. It is noticed that the SRT feeding network usually has a complex structure, which is not convenient for antenna systems integration. To reduce the size of the feed network, a sequential phase (SP) feeding technique with single transition line has been massively investigated due to its advantage of magnitude and phase control. Over years, a proximity-coupled feeding method has been used to broaden the CP bandwidth in [7]–[15], which

can provide equal magnitude and stable 90° phase difference at four ports. Reference [13] designs a broadband CP MPA which employs the SP feeding structure to the CP elements through aperture coupling, which needs three substrate layers. By combining parasitic loops with 90° phase-delay line, a novel crossed dipole CP antenna [14] with a broad ARBW of 28.6% is proposed. In [15], a CP shorted loop is used as the SP feeding structure in a sequential-rotation CP patch array design, which can achieve 7% ARBW. However, this proximity-coupled method needs at least two dielectric layers, which increases the antenna profile. To solve this problem, a series-parallel feeding structure [16]–[22] has been introduced into CP MPA designs. In [16]–[17], two differently series-parallel feeding structures are applied to a sequential-rotation patch array, which obtains narrow 4.8% and 5.4% ARBW, respectively. For the purpose of broadening the CPBW, a single-layer wideband CP 2 × 2 patch array with an ARBW of 12.7% is proposed through utilizing a square-loop SP rotated structure in [18]. Similarly, based on this square-loop feeding structure, various of coupled elements are often placed at the edge of the feeding structure to increase the CPBW in [19]–[22], such as circular radiation patch (6.7%) [19], four parasitic rectangular elements (15.9 %) [20], four square driven patches and four parasitic square patches (12.9 %) [21], and an L-shaped parasitic patch (28.1 %) [22].
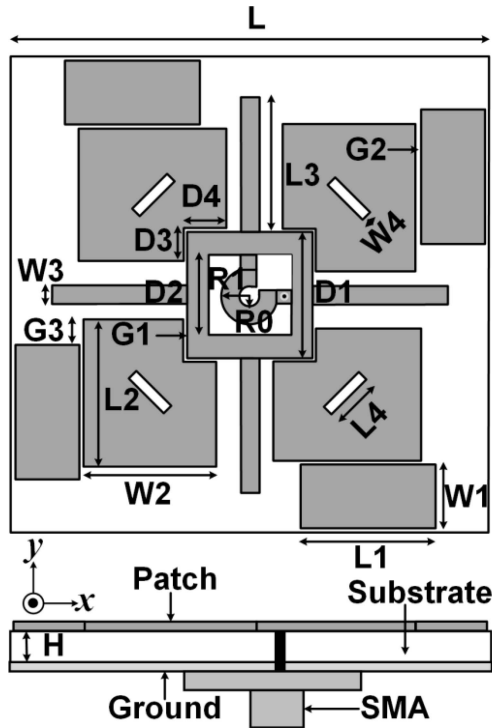
FIGURE 1. The geometry of the proposed antenna.

FIGURE 2. Five antenna structures in the design process.

TABLE 1. The geometrical parameters of the proposed antenna.

Parameters	Values	Parameters	Values
L	50 mm	H	1.524 mm
L1	14 mm	W1	6.6 mm
L2	15.3 mm	W2	13.95 mm
L3	14 mm	W3	2.0 mm
L4	5.12 mm	W4	1.0mm
D1	13.1 mm	D2	8.68 mm
D3	4.4 mm	D4	3.45 mm
R0	1.0 mm	R1	3.0 mm
G1	0.1 mm	G2	0.8 mm
G3	2.9 mm		

the square-loop is designed through cutting off a square (D2 × D2) from a square (D1 × D1). In addition, an arc-shaped strip is arranged inside the square-loop to stimulate 90° phase difference. The inner and outer radius of the strip are R0 and R1, respectively. The ANSYS HFSS 18.0 is utilized to determine the final dimensions of the MPA, which are listed in Table 1.

B. ANTENNA OPERATING MECHANISM

To explain the operating mechanism of the proposed antenna clearly, five models (Ant. I to Ant. V) with progressive design process are shown in Fig. 2. The corresponding return loss and AR curves of these models are depicted in Fig. 3(a) and Fig. 3(b), respectively. The Ant. I has a SP square-loop feeding structure with four L-shaped patches. For a traditional square-ring antenna, the resonance frequency of basic mode (TM_{11} mode) is determined by the average circumference of the square-ring, which can be expressed as [16]

$$f_{11} = \frac{c}{2(D1 + D2)} \times \left(\frac{1 + \varepsilon\varepsilon_r}{2\varepsilon_r} \right)^{1/2} \quad (1)$$

where c represents the speed of light, D1 and D2 are the inner and outer length of the square-ring respectively, 2(D1 + D2) is the average circumference of the square-loop, εr represents the dielectric constant of the medium. The arc-shaped strip can generate stable 90° phase difference due to its length is a quarter of the waveguide wavelength at 6.35 GHz. When a square-loop is arranged outside the strip, one wavelength and sequential phases of 0°, 90°, 180° and 270° could be achieved simultaneously on the square-loop.

As shown in Fig. 3, Ant. I with four parasitic L-shaped patches produces two resonant modes (f1 and f2) due to effect of perturbation. The two resonances can be separately controlled by the square-loop feeding structure and L-shaped patches. When I-slot is inserted into the L-shaped

---

Based on the previous investigations on CP MPA with the SP feeding structure, a compact wideband CP MPA with a square-loop SP feeding structure is proposed in this work. The antenna consists of a CP square-loop with sequential phase characteristics, four strip-lines as driven elements, four L-shaped patches with I-slots and four I-shaped patches as parasitic elements. Firstly, a square-loop is designed as a SP feeding structure. Secondly, four strip-lines are utilized to generate one CP mode by a directed connection. Thirdly, in order to broaden the low frequency bandwidth, four parasitic L-shaped patches are inserted by a capacitively coupled way. Finally, the high frequency bandwidth can also be broadened by introducing four parasitic I-shaped patches. By combining these structures, multiple CP modes can be generated to realize wideband CP operation. The presented antenna has a wide 3-dB ARBW of 18.9% (6.35 GHz, 5.75-6.95 GHz), and a wide 10-dB IBW of 23% (6.38 GHz, 5.65-7.12 GHz).

II. ANTENNA DESIGN
A. ANTENNA CONFIGURATION
The detailed geometry of the presented CP MPA with the SP circular-loop feeding structure is plotted in Fig. 1. The MPA is etched on a 1.524-mm thick Rogers 5880 substrate (εr = 2.2 and tanδ = 0.002). The antenna consists of two pairs of parasitic elements that are placed outside a SP square-loop feeding structure, which is directly connected with a 50-Ω coaxial cable. The L-shaped parasitic elements include four L-shaped patches (L2 × W2), and four I-shaped slots (L4 × W4). The dimension of four I-shaped patches is L1 × W1. In order to obtain stable phase difference,

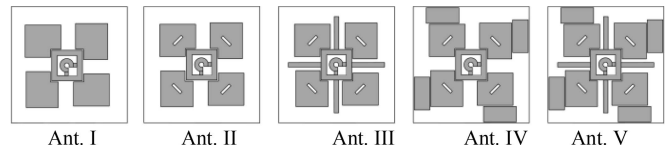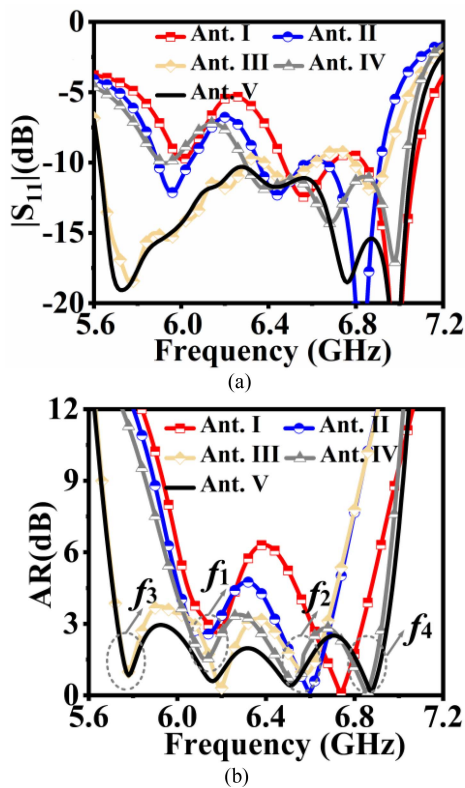**FIGURE 3.** $|S_{11}|$ and AR curves for different antennas, (a) $|S_{11}|$ curves (b) AR curves.

FIGURE 4. The corresponding ARs and $|S_{11}|$ with various parameters: (a) L1, (b) L2, and (c) L3.

patch, the IBW and ARBW of Ant. II could be improved well. For Ant. III, it is observed that when four strip-lines are directly connected with the square-loop, a new resonant mode (f3) is excited in the low frequency. Similarly, based on the Ant. II, when four I-shaped patches are placed next to the L-shaped patches (Ant. IV), a new resonant mode (f4) occurs in the high frequency. In summary, four driven strip-lines and four I-shaped patches excite low-frequency resonance mode (f3) and high-frequency resonance mode (f4), respectively. Thus, multiple CP modes (Ant. V) could be stimulated to meet the requirement of the wideband CP radiation by combining these driven strip-lines with parasitic elements. Eventually, the proposed CP MPA realizes a wide 10-dB IBW of 22.1% from 5.63-7.05 GHz and a 3-dB ARBW of 19.2% (5.73-6.95 GHz). Moreover, comparing with previous CP antenna, the presented antenna has a wider CPBW (18.9%) and a compact structure, which is listed in Table 2.

C. ANTENNA PARAMETER ANALYSIS

To investigate the effect of the antenna sizes on the CP performance, a parameter study is conducted. Here, the dimension of the I-shaped patches (L1), the dimension of the L-shaped patches (L2), and driven strip-lines (L3) are analyzed by HFSS. The corresponding ARs and $|S_{11}|$ are plotted in Fig. 4. It is observed that the ARs and $|S_{11}|$ change greatly with different L1 and L3 in the higher frequency
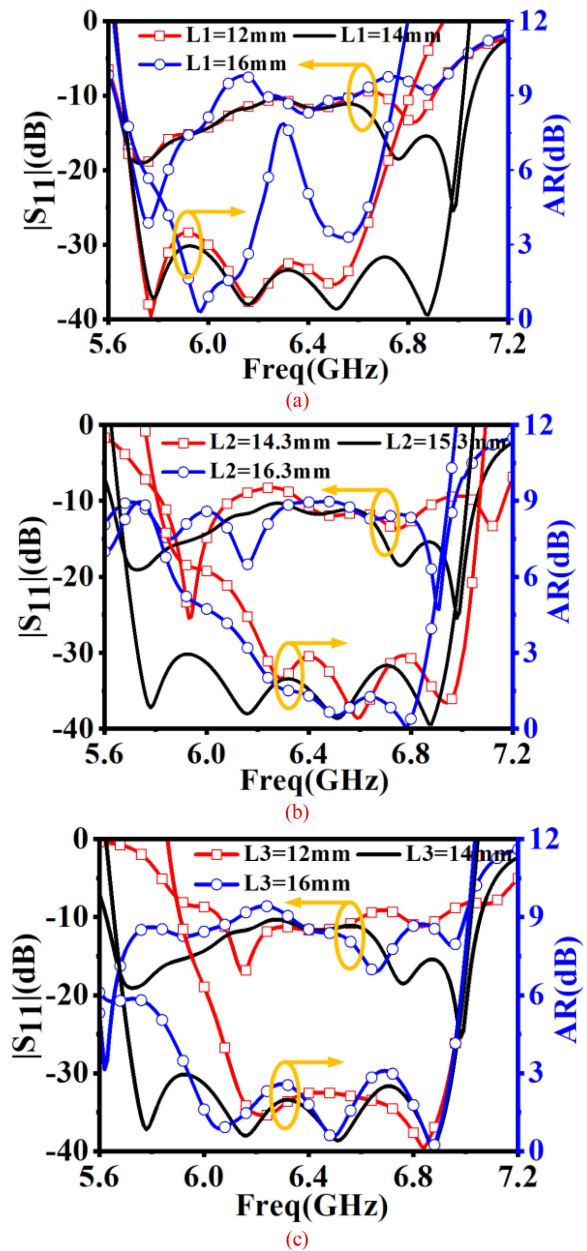
(f_4) and lower frequency (f_3) respectively, which are consistent with the results of Fig. 3. We can also see that the ARs and $|S_{11}|$ vary dramatically with different L2 in the low frequency (f_1 and f_3). This is because that the resonant mode (f_1) is generated by the L-shaped patches. Besides, due to the vary of L2 causing the coupling energy change from the L-shaped patches to I-shaped patches, the resonant mode (f_3) also changes with different L2. When L1 = 14, L2 = 15.3, and L3 = 16mm, the widest ARBW and IBW can be obtained. Finally, the comparison between the proposed and the published CP microstrip antennas is shown in Table 2, indicating that the antenna has a wider CP performance.
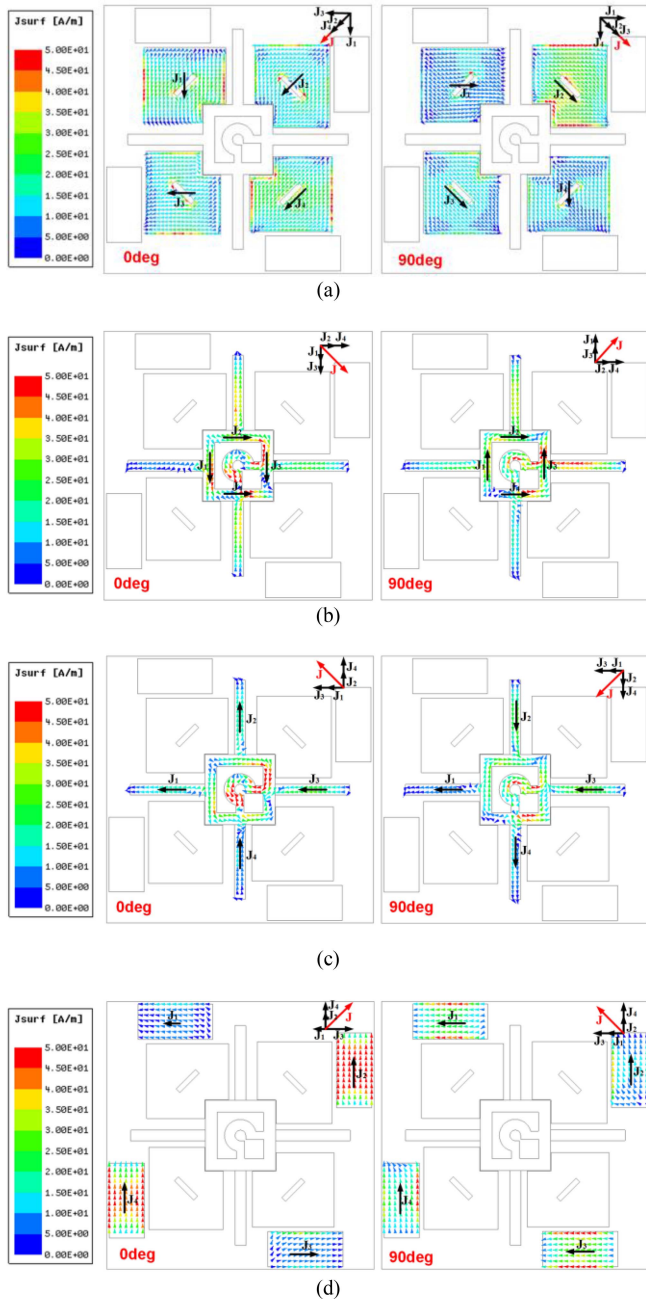
FIGURE 5. Simulated current distributions on the MPA with the phases of 0° and 90° at (a) 6.15 GHz, (b) 6.5 GHz, (c) 5.8 GHz and (d) 6.9 GHz, respectively.

FIGURE 6. Simulated and measured $|S_{11}|$ and AR results of the antenna.

TABLE 2. Comparison of the proposed antenna to previously reported antennas.

Ref	Type	Antenna Size	IBW (%)	AR BW (%)	Peak gain (dBi)
[14]	Double layered	$1.67 \lambda_0 \times 1.67 \lambda_0 \times 0.058 \lambda_0$ at 5.0GHz	6	6.8	10.5
[17]	Single layered	$1.16 \lambda_0 \times 1.16 \lambda_0 \times 0.013 \lambda_0$ at 2.5GHz	8	4.8	7.5
[18]	Single layered	$1.38 \lambda_0 \times 1.38 \lambda_0 \times 0.028 \lambda_0$ at 5.5GHz	18	12.7	12
[20]	Single layered	$1.47 \lambda_0 \times 1.47 \lambda_0 \times 0.028 \lambda_0$ at 5.5GHz	15.8	11.8	12.5
[21]	Single layered	$0.92 \lambda_0 \times 0.92 \lambda_0 \times 0.028 \lambda_0$ at 5.5GHz	19.5	12.9	9.8
[22]	Double layered	$0.80 \lambda_0 \times 0.80 \lambda_0 \times 0.076 \lambda_0$ at 5.6 GHz	38	28.1	8.4
Proposed	**Single layered**	**$1.06 \lambda_0 \times 1.06 \lambda_0 \times 0.03 \lambda_0$ at 6.35GHz**	**23**	**18.9**	**10.2**

To reveal the CP working mechanism, the simulated current distributions with two different time phases of 0° and 90° are shown in Fig. 5. After comparing and analyzing the AR resonance points of different antennas from Fig. 3 and Fig. 4, we choose the surface currents on the L-shaped patches at 6.15 GHz, the square-loop at 6.6 GHz, the I-shaped strips at 5.8 GHz, and the I-shaped patches at 6.9 GHz to study the CP operating mechanism, respectively. The reason why we plot the surface currents on these elements is that they excite different circular polarization modes at different frequencies, respectively. As seen from Fig. 5,
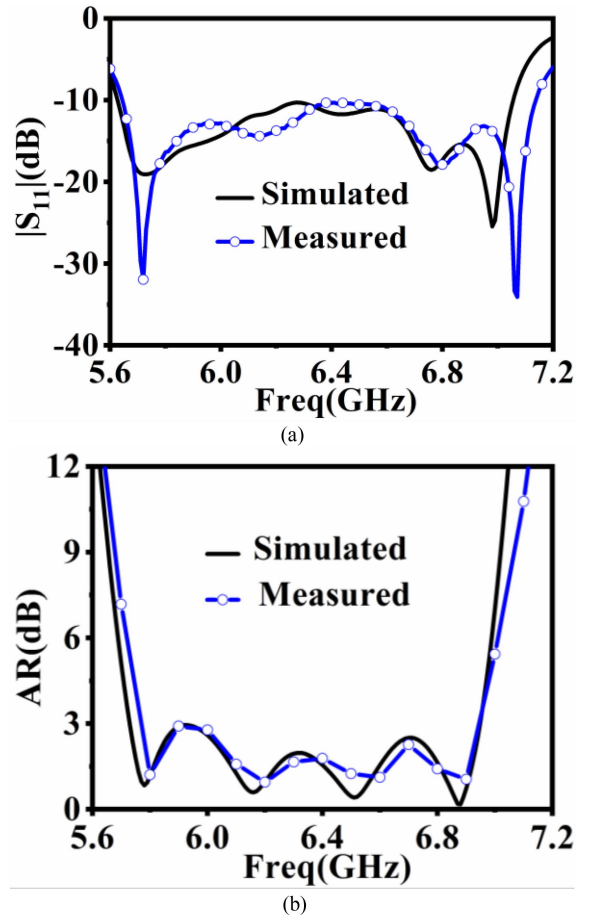
the surface currents on these elements in 0° and 90° are about equal in magnitude and 90° difference in phase, and sequentially rotate counterclockwise with different phases, which means the antenna radiates right-hand circularly polarized (RHCP) waves in +z-direction. The analysis results of surface current distributions are consistent with the simulated results of five progressive models in Fig. 2 and Fig. 3. Therefore, the CP bandwidth of the proposed antenna could be greatly enhanced by utilizing these parasitic patches.
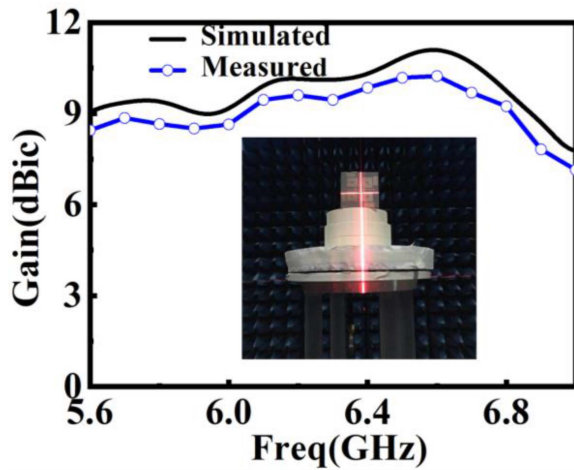
FIGURE 7. Measurement and simulation d antenna gains and test photograph.

TABLE 3. Simulated and measured power beamwidths of the proposed antenna.

Frequency (GHz)	Simulated 3-dB power beamwidth		Measured 3-dB power beamwidth	
	xoz-plane	*yoz*-plane	*xoz*-plane	*yoz*-plane
5.8	53°	55°	51°	58°
6.2	54°	55°	47°	57°
6.6	44°	43°	48°	51°

III. EXPERIMENTAL RESULTS

To verify the simulated results, an optimal prototype of the presented CP MPA was manufactured and tested. This antenna is measured by a vector network analyzer (AgilentN5224A). Fig. 6 illustrates the comparison between the measurement and simulation results with frequency. As shown in the picture, the measured and simulated 10-dB IBW are 5.65-7.12 GHz (23%) and 5.63-7.05 GHz (22.1%) respectively. Correspondingly, the 3-dB ARBW are 5.75-6.95 GHz (18.9%) and 5.73-6.95 GHz (19.2%). Fig. 7 displays measurement and simulation antenna broadside gains and photograph of antenna test, the tested gains are greater than 8.4 dBic in the 3-dB ARBW and the peak gain is 10.2 dBic. The normalized radiation patterns of the proposed CP MPA at 5.8, 6.2 and 6.6 GHz (xoz-plane and yoz-plane) are presented in Fig. 8. It is obviously observed that the CP MPA can stimulate the RHCP at 5.8, 6.2 and 6.6 GHz in +z-direction. In addition, the simulated and measured half power beamwidths at different frequencies are shown in Table 3. The simulation and measurement results are not exactly same. This is because that the feeding cable and the SMA connector have obvious impact on the measurement results, which are not considered in the simulation model. Eventually, measurement and simulation results together validate the rationality of the presented design.

IV. CONCLUSION

A new compact broadband CP MPA is proposed in this work. The antenna consists of a CP square-loop with
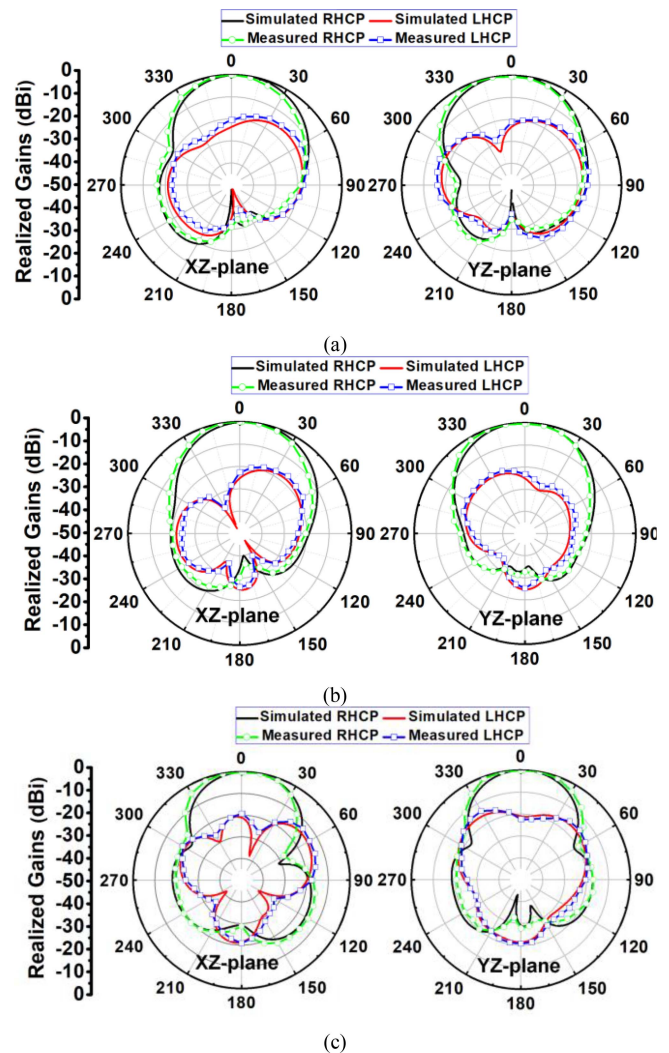

FIGURE 8. Measurement and simulation antenna radiation patterns at (a) 5.8 GHz, (b) 6.2 GHz, and (c) 6.6 GHz.

SP characteristics, four strip-lines as driven elements, four L-shaped patches with I-slots and four I-shaped patches as parasitic elements. By combining these structures, multiple CP modes can be generated to realize wideband CP operation. Eventually, the presented antenna has a wide 3-dB ARBW of 18.9% (6.35 GHz, 5.75-6.95 GHz), and a wide 10-dB IBW of 23% (6.38 GHz, 5.65-7.12 GHz). Besides, the presented antenna features flat gain within the CP operation bandwidth and compact structure.

REFERENCES

[1] E. Arnieri, L. Boccia, G. Amendola, and G. D. M. Massa, "A compact high gain antenna for small satellite applications," *IEEE Trans. Antennas Propag.*, vol. 55, no. 2, pp. 277–282, Feb. 2007.

[2] H. L. Chung, X. Qing, and Z. Ning, "Broadband circularly polarized stacked patch antenna for UHF RFID applications," in *Proc. IEEE Antennas Propag. Soc. Int. Symp.*, Honolulu, HI, USA, 2007, pp. 1189–1192.

[3] P. S. Hall, "Application of sequential feeding to wide bandwidth, circularly polarised microstrip patch arrays," *IEE Proc. H-Microw. Antennas Propag.*, vol. 136, no. 5, pp. 390–398, Oct. 1989.

[4] D. F. Guan, C. Ding, Z. P. Qian, Y. S. Zhang, Y. J. Guo, and K. Gong, "Broadband high-gain SIW cavity-backed circular-polarized array antenna," *IEEE Trans. Antennas Propag.*, vol. 64, no. 4, pp. 1493–1497, Apr. 2016.

[5] A. Chen, Y. Zhang, Z. Chen, and C. Yang, "Development of a *Ka*-band wideband circularly polarized 64-element microstrip antenna array with double application of the sequential rotation feeding technique," *IEEE Antennas Wireless Propag. Lett.*, vol. 10, pp. 1270–1273, 2011.

[6] M. Li and K.-M. Luk, "Low-cost wideband microstrip antenna array for 60-GHz applications," *IEEE Trans. Antennas Propag.*, vol. 64, no. 4, pp. 3012–3018, Jun. 2014.

[7] R. R. Ramirez, F. Flaviis, and N. G. Alexopoules, "Single-feed circularly polarized microstrip ring antenna and arrays," *IEEE Trans. Antennas Propag.*, vol. 48, no. 7, pp. 1040–1047, Jul. 2002.

[8] H. Iwasaki, "A circularly polarized rectangular microstrip antenna using single-fed proximity-coupled method," *IEEE Trans Antennas Propag.*, vol. 43, no. 8, pp. 895–897, Aug. 1995.

[9] W. K. Lo, K. M. Luk, and C. H. Chan, "Circularly polarised microstrip antenna array using proximity coupled feed," *Electron. Lett.*, vol. 34, no. 23, pp. 2190–2191, Nov. 1998.

[10] W. K. Lo, C. H. Chan, and K. M. Luk, "Circularly polarised patch antenna array using proximity-coupled l-strip line feed," *Electron. Lett.*, vol. 36, no. 14, pp. 1174–1175, Jul. 2000.

[11] J.-W. Wu and J.-H. Lu, "2×2 circularly polarized patch antenna arrays with broadband operation," *Microw. Opt. Technol. Lett.*, vol. 39, no. 5, pp. 360–363, 2003.

[12] L. Bian and X. Q. Shi, "Wideband circularly-polarized serial rotated 2×2 circular patch antenna array," *Microw. Opt. Technol. Lett.*, vol. 49, no. 12, pp. 3122–3124, 2007.

[13] Y. Lu, D. G. Fang, and H. Wang, "A wideband circularly polarized 2×2 sequentially rotated patch antenna array," *Microw. Opt. Technol. Lett.*, vol. 49, no. 6, pp. 1405–1407, 2007.

[14] Y. Li, Z. Zhang, and Z. Feng, "A sequential-phase feed using a circularly polarized shorted loop structure," *IEEE Trans. Antennas Propag.*, vol. 61, no. 3, pp. 1443–1447, Mar. 2013.

[15] J.-W. Baik, T.-H. Lee, S. Pyo, S.-M. Han, J. Jeong, and Y.-S. Kim, "Broadband circularly polarized crossed dipole with parasitic loop resonators and its arrays," *IEEE Trans Antennas Propag.*, vol. 59, no. 1, pp. 80–88, Jan. 2011.

[16] A. Chen, Y. Zhang, Z. Chen, and S. Cao, "A *ka*-band high-gain circularly polarized microstrip antenna array," *IEEE Antennas Wireless Propag. Lett.*, vol. 9, pp. 1115–1118, 2010.

[17] S.-K. Lin and Y.-C. Lin, "A compact sequential-phase feed using uniform transmission lines for circularly polarized sequential-rotation arrays," *IEEE Trans. Antennas Propag.*, vol. 59, no. 7, pp. 2721–2724, Jul. 2011.

[18] C. Deng, Y. Li, Z. Zhang, and Z. Feng, "A wideband sequential-phase fed circularly polarized patch array," *IEEE Trans. Antennas Propag.*, vol. 62, no. 7, pp. 3890–3893, Jul. 2014.

[19] Y.-Q. Zhang, S.-T. Qin, X.-W. Wang, and F. Shang, "Novel single-fed broadband circularly polarized antenna for GNSS applications," *Int. J. RF Microw. Comput.-Aided Eng.*, vol. 28, no. 7, 2018, Art. no. e21193.

[20] K. Ding, C. Gao, T. Yu, D. Qu, and B. Zhang, "Gain-improved broadband circularly polarized antenna array with parasitic patches," *IEEE Antennas Wireless Propag. Lett.*, vol. 16, pp. 1468–1471, 2017.

[21] K. Ding, C. Gao, D. Qu, and Q. Yin, "Compact broadband circularly polarized antenna with parasitic patches," *IEEE Trans. Antennas Propag.*, vol. 65, no. 9, pp. 4854–4857, Sep. 2017.

[22] W.-W. Yang, W.-J. Sun, W. Qin, J.-X. Chen, and J.-Y. Zhou, "Broadband circularly polarised stacked patch antenna with integrated dual-feeding network," *IET Microw. Antennas Propag.*, vol. 11, no. 12, pp. 1791–1795, Sep. 2017.

[23] K.-L. Wong, C.-C. Huang, and W.-S. Chen, "Printed ring slot antenna for circular polarization," *IEEE Trans. Antennas Propag.*, vol. 50, no. 1, pp. 75–77, Jan. 2002.

[24] X. Chen, G. Fu, S.-X. Gong, Y.-L. Yan, and W. Zhao, "Circularly polarized stacked annular-ring microstrip antenna with integrated feeding network for UHF RFID Readers," *IEEE Antennas Wireless Propag. Lett.*, vol. 9, pp. 542–545, 2010.

LEI WANG (Member, IEEE) was born in Shaanxi, China, in 1991. He received the B.S. degree and M.S. degree in electromagnetic field and microwave technology from Xidian University, Xi'an, China, in 2017. He joined China Electronic Produce Reliability and Environmental Testing Research Institute, Guangzhou, China, and severed as an Engineer. His research interests include electromagnetic compatibility and design of circularly polarized microstrip antennas.

YUN-FEI EN (Senior Member, IEEE) received the B.S. degree in semiconductor physics and solid state electronics in 1990, and the M.S. degree in semiconductor devices and microelectronics and the Ph.D. degree from Xidian University in 1995 and 2013, respectively. Since 1995, she has been with the China Electronic Produce Reliability and Environmental Testing Research Institute. She worked on the failure mechanism and reliability evaluation of components. Since 2006, she has been serving as a Research Fellow with the Science and Technology on Reliability Physics and Application of Electronic Component Laboratory. She has authored or coauthored five books and more than forty scientific publications in journals and international conferences. Her research interests include electromagnetic compatibility, microelectronics, and failure analysis of electronic components.